International Research Journal of Advanced Engineering and Science
ISSN (Online): 2455-9024

Pre-Drill Pore Pressure Prediction from Seismic Velocities: A Case Study of Agbada Field in Niger Delta, Nigeria

J. U. Okey[1], O. A. Davies[1], V. Baatee[1]
[1]Physics Department, Rivers State University, Port Harcourt, Rivers State, Nigeria

Abstract— *This research was carried out in the Agbada Field in the Central Swamp area of the Niger Delta Petroleum basin. Well-log and seismic data were used to predict pre-drill pore pressure in the subsurface rock matrix. Variables estimated from the offset well included overburden gradient, shale pore pressure and fracture gradient. While those estimated from the seismic data included seismic velocities, pore pressure and fracture gradient. Mild overpressures were encountered in the calibration well from 10,800ftss to 11,702ftss where pressures of between 0.5 and 0.51 psi were observed. Hard overpressures of between 0.77 and 0.81psi were also seen from 13,318ftss to the bottom of the well at 14,502ftss. Vertical effective stress reversal which is also an indicator of overpressure was observed at 11,702ftss. Another indicator of overpressure, overburden pressure, increased from 11,800ftss as well, and a corresponding fracture gradient also increased at 14000ftss. While the total drilled depth of the calibration well was 14,508ftss, the total sampled depth of the seismic velocities was more than 18000ftss (about 5000ms). The seismic derived fracture gradient increased between 2800ms and 3000ms (about 13,800ftss) in agreement with that calculated from the calibration well. Vertical effective stress reversal was also observed between 2500ms and 3,500ms (10,000ftss – 14,000ftss), just as was observed in the well. Overburden pressure dropped between 2800ms and 3000ms. This was also confirmed from the well results. Mild overpressures were predicted from 2500ms to 2650ms (10,00ftss to 10,700ftss) and hard overpressure from 2700ms to 3100ms (11,000ftss to 13,200ftss). Seismic velocity and well-log data were in good agreement for the pore pressure profile of the calibration well.*

Keywords— *Pore Presure, Fracture Gradient, Overpressure, Seismic Velocities, Well log, Overburden Gradient.*

I. INTRODUCTION

Hydrocarbon exploration and production is steadily moving away from familiar onshore environments due to rapidly depleting resources and security challenges, to deep and ultra-deep-water environments which are believed to hold tremendous prospects for our future energy needs [1, 2]. The conditions for the existence of abnormal pore pressures are usually rife in these types of environments [3]. Therefore, an accurate prediction of pore pressure and fracture gradient have become essential to the drilling of wells in these areas. Abnormal pore pressures are encountered worldwide, often resulting in drilling problems such as kicks, blowouts, borehole instability, stuck pipe and loss of circulation [4].

Generic subsurface pore pressure profile is usually described as unconfined (the shallow zone), hydrodynamic the middle zone) and over-pressured (the lower zone) [5]. The shallow unconfined zone exists below the mud line to the depth where compaction disequilibrium dewatering process (CDD) commences. This zone is usually subject to free flow surface water. In offshore environment, sea level fluctuation, brackish water encroachment and sediments influx directly impacts the hydrostatic behaviour of the normally pressured system [6, 7]. The middle zone lies between the CDD and the fluid retention depth (FRD), also known as top of geopressure (overpressure). Here, upward dewatering process takes place, a result of the gradual pressure gradient drop from the deep to the shallow layers [8]. The fluid retention depth is the depth where dewatering is stops [7]. It is also referred to as top of geopressure (TOG). This zone can be referred to as the transition zone (TZ) between normally pressured upper unconfined zone and over-pressured lower zone. Drilling water flow hazards are common in this zone among young deep-water sediments. These hazards are usually initiated by the vertical flow generated by the pressure differential and permeability contrast in this zone [9]. In this transition zone, pore fluids are gradually expelled from sediments due to pressure gradient drop from deeper to shallower zones [7]. The resultant effect is that the measured petrophysical parameters like velocity, density and resistivity continue to increase downward concurrent with the rate of dewatering process. The lower confined section is the geopressured or overpressured zone where the pore pressure gradient exceeds the expected hydrostatic pressure gradient [7]. Although sand beds (reservoirs) show a hydrostatic pressure gradient in this section, pressure gradient in shale (seals) is higher and tends to be analogous to the principal stress (overburden pressure) gradient. According to Shaker and Reynolds [10], drilling in the geopressured section requires several casing points contingent on the subsurface drilling tolerance window. In this section, because water is no longer capable of escaping, velocity, density, and resistivity measurements retreat in the seals [7, 10],

Geophysical techniques in conjunction with other related tools can provide the means of predicting pore pressure. These techniques are based on the impact of reservoir pressure on seismic velocities (primarily compressional waves). Pore pressure can therefore be predicted from seismic velocities, using a suitable velocity to pore pressure transform calibrated with data obtained from offset wells in the area [11, 12, 13]. Changes in pore pressure can also be recognized on regular formation evaluation tools such as sonic, resistivity, porosity,

ISSN (Online): 2455-9024

and density logs [4, 14]. These logs show the effects of pore pressure because of the relationship between compaction, porosity, density, and the electrical and acoustic properties of sediments. As a rock compacts, the porosity is reduced and the density increases, which also causes the bulk modulus and shear modulus to rise because of increases in grain contact area and grain contact stress [15]. This process continues until the mechanical process of compaction is slowed by either the stiffness of the rock frame or by increases in pore pressure that resist further compaction.

This research is therefore designed to predict pre-drilling pore pressure from seismic and well log data from Agbada Field in the Niger Delta region of Southern Nigeria.

II. THE STUDY AREA

This research was carried out with data obtained from Agbada Field in the Central swamp area of the Niger Delta Petroleum basin. The Niger Delta is a low gradient tertiary delta approximately 211,000km^2 in surface area and developed south-westwards out of the Anambra Basin and the Benue Trough [16, 17]. It lies south of the West African shield and west of the Oban Massif and the Tertiary Cameroun Volcanic trend. The delta is located east of the Benin basin and its southern margin is marked by seafloor escarpments that lie over the oceanic crust [18].

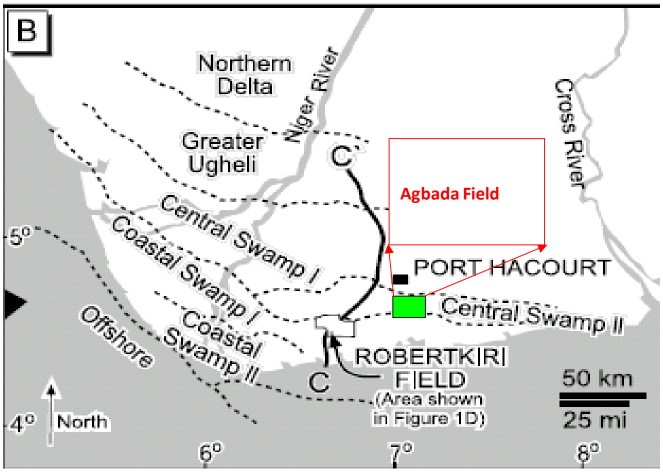

Fig. 1: Map of the Niger Delta showing the Study Area [19]

III. MATERIAL AND METHOD

A. Data Acquisition

The data used in this research was sourced from the Nigerian National Petroleum Corporation (NNPC) and one of its major joint venture partners, with the permission of the Directorate of Petroleum Resources. The seismic data used, came from the Okpodon 3D pre stack depth migrated volume which has a total subsurface coverage of 500 square kilometer, encompassing the study area. The Okpodon 3D PSDM volume was acquired in 1993 using a brick wall pattern, with a nominal fold of 16. And the well data which includes well logs, checkshots, Leak-off test and RFT measurements came from Agbada well 060 which was drilled to test deep prospects between 12,100 to 15,500ft below the Okpodon field.

B. Well Log Editing, Conditioning and Checkshot Inversion

Relevant well logs and checkshots were obtained from the calibration well, quality-checked and conditioned, to minimize errors resulting from washout, cycle skip, rugosity and alteration due to prolonged periods of exposure to drilling fluids. These effects are usually common with density and sonic logs. Calibrating sonic logs with checkshot can considerably increase their reliability and usability [20]. Accurate and continuous sonic and density logs are fundamental to pore pressure prediction [21].

About four checkshot surveys were carried out in the area, but the checkshot of Well A was used because it was deeper and more reliable. Interval velocities were calculated from checkshots using the following relation according to Robinson and Coruh [22];

$$V_i = \frac{Z_i - Z_{i-1}}{t_i - t_{i-1}} \tag{1}$$

Where Z_i is the given depth, Z_{i-1} is the preceding depth, t_i is a given time while t_{i-1} is the preceding time.

C. Identifying and Picking of Shale Intervals

Shale intervals were identified from gamma ray logs and from sand tops and bases. Shale volume log was modelled from gamma ray log using the volume tract generator in RokDoc proprietary software. The Shale trend velocity log was then generated using the calibrated sonic log and the shale volume log as input.

D. Generation of Overburden Gradient from Offset Well Density Data

The overburden gradient, S, was calculated from an integral of density courtesy of Sayers [4] as follows

$$S = g\int_0^z \rho(z)dz \tag{2}$$

Where $\rho(z)$ is the density at depth z below the surface and g is acceleration due to gravity.

E. Estimation of Shale Pore Pressure and Fracture Gradient at Offset Well

Eaton's [23] effective stress model for transforming velocity to pore pressure was applied to obtain a profile of shale pore pressure at the offset well according to the relationship;

$$PP = S - (S - H) \times \left(\frac{V_{Obs}}{V_{Norm}}\right)^N \tag{3}$$

Where PP is the pore pressure gradient in psi/ft at the offset well, S is the overburden stress gradient, H is the hyrostatic pressure gradient (taken to be $0.44 psi/ft$ for the study area), V_{obs} is the sonic velocity reading taken from the well log and V_{Norm} is the velocity expected in a normally pressure shale interval (values of V_{Obs} and V_{Norm} were read off the shale trend velocity log and the NCT velocity log), N is Eaton's exponent, which is a transformational exponent and is variable with basin type and its age. It describes the sensitivity of velocity to effective stress. In the Niger delta, the exponent has a value of 3, which is typical for young clastic tertiary basins like the Niger delta and the Gulf of Mexico [24].

Furthermore, the fracture gradient, FG, was as derived from Eaton's [23] relationship;

$$FG = k \times (PS - PP) + PP \quad (4)$$

Where PS is the overburden stress and k is the ratio of horizontal to vertical stress, estimated from Poisson's ratio and gamma ray log for uniaxial strain (since we are dealing with strain only in the vertical direction here) such that;

$$PP = \frac{\mu}{1 - \mu} \quad (5)$$

Where μ is Poisson's ratio, which was estimated as;

$$\mu = 0.125 I_{GR} + 0.27 \quad (6)$$

Where I_{GR} is gamma ray index determined from gamma ray log according to [25];

$$I_{GR} = \frac{GR_{log} - GR_{min}}{GR_{max} - GR_{min}} \quad (7)$$

Where GR_{log} is the gamma ray reading at the depth of interest, GR_{min} is the minimum gamma ray reading and GR_{max} is the maximum gamma ray reading.

Additionally, the vertical effective stress (VES_{offset}) was estimated from the difference between overburden stress (PS) and pore pressure (PP), as given by Terzaghi [26];

$$VES_{offset} = PS - PP \quad (8)$$

F. Extraction of Seismic Velocities

Seismic interval velocities extracted from the Okpodon3D seismic data were available as a function of time on a grid of 200m by 200m spacing, but they were not suitable for pore pressure prediction because they were over-smoothed. A new fit-for-purpose velocity model was generated on a grid of 100m by 100m from the available RMS velocities for the area of interest. A total of 494 velocity analysis points were picked around the offset well and the proposed drilling location. The picked RMS velocities were then converted to interval velocities via Dix equation [27];

$$V_{INT} = \sqrt{\frac{V_n^2 T_n - V_{n-1}^2 T_{n-1}}{T_n - T_{n-1}}} \quad (9)$$

where V_{INT} is interval velocity, while T_n is the zero-offset arrival time corresponding to the n^{th} reflection. V_n is the root-mean-square velocity. The interval velocities were then calibrated with well data to yield the final earth velocity model, which was used for the pore pressure prediction.

G. Caliberation of Seismic Velocities

The calibration procedure involves the generation of a set of transforms that are used to scale the seismic velocities for them to see the earth just the way the control well sees it. The key steps in the process are outlined below:

- Scale the checkshots using the offset well sonic logs by applying a calibration factor derived from the crossplot of sonic log and the checkshot-derived interval velocity.
- Calculate checkshot time as an integral over depth from the surface to the depth of interest.
- Calculate depth as a function of time.
- To minimize the mismatch between the original and the checkshot depths, error analysis was carried out and the results optimized using the Excel solver analysis. The calibration of the checkshots with sonic logs was necessary because checkshots derived velocities and sonic velocities have different wavelengths and frequencies of propagation, therefore they could be significant depth errors when recalibrating to seismic lines.
- The original seismic data did not extrapolate through (0 0), hence arbitrary zeros were taken as new surface values. The equivalent surface depth was then calculated from checkshot fit and the subsequent depths were derived by summation from the surface down to the points of interest.
- Interval velocity was also calculated from seismic data, with the results optimized as well.
- The initial seismic depth from the surface is assumed to be the same with that of the checkshot fit, while the subsequent depth was calculated.
- Calculate fitted time and carry out error analysis as was done with the checkshot data, but in this case the depth being integrated comes from the calculated seismic depth.
- Estimate transform intercept and transform slope.
- A calibrated seismic depth that aligns with the checkshot depth, within acceptable limits of errors was calculated in much the same manner as the fitted checkshot depth, but with the input parameters coming from the raw seismic time and fitted seismic time.

H. Prediction of Pore Pressure from Seismic Velocity

The effective stress model for transforming seismic velocities to pore pressure in shale is based on the following relation as given by Terzaghi [26];

$$PP = OBP - VES \quad (10)$$

Where PP is pores pressure gradient, OBP is the overburden pressure gradient and VES is the vertical effective stress gradient. The two unknown parameters must therefore be determined, for pore pressure to be predicted.

To estimate the VES from seismic velocity, the first step is to cross plot the offset well VES_{offset} against the modeled shale trend velocity as shown in figure 2. The subsequent regression equation is then used with the calibrated seismic velocity to derive the VES profile of the area of interest, from the seismic data.

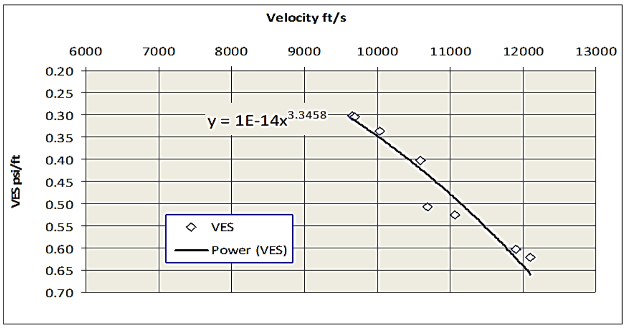

Fig. 2: Velocity versus Offset Well Vertical Effective Stress (VES) Gradient.

The overburden pressure (OBP), in psi/ft, was derived from the calibrated seismic velocity using Gardner's equation [28];

$$OBP = 0.433 \times aV^b \quad (11)$$

International Research Journal of Advanced Engineering and Science
ISSN (Online): 2455-9024

Where a and b are constants that are consistent with basin type and age of the sediments, V is calibrated seismic velocities. In the study area, by doing a cross plot of density and the modeled shale trend velocity from the calibration well and fitting a power curve into the data points from which a regression equation was derived, a and b values were found to be 0.068 and 0.382 respectively.

I. Prediction of Fracture Gradient from Seimic

The fracture gradient is a function of the overburden pressure, vertical effective stress and pore pressure [29]. It was also predicted from the seismic velocities according to [30] as follows;

$$FG = P + 0.5VES \qquad (12)$$

where P is the pore pressure gradient (derived from seismic velocity), 0.5 represents the Poisson's ratio for wet shale and VES is the vertical effective stress (derived from seismic velocity).

IV. Results and Discussions

A. Results

The relevant results obtained from the methodology employed during this research are displayed below.

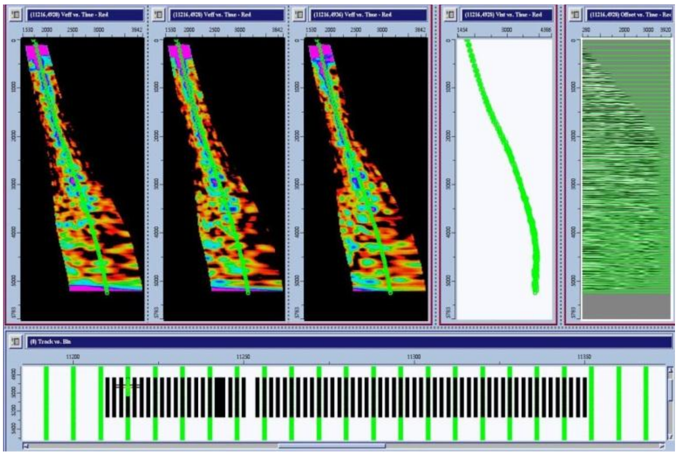

Fig. 3: Semblance Panel Velocity versus Time Display for Velocities extraction from Seismic Volume

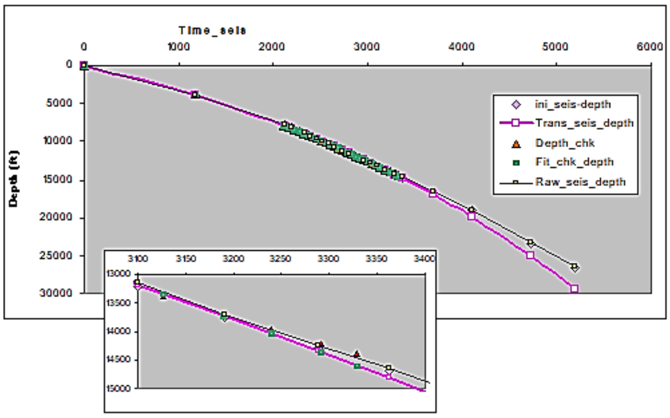

Fig. 4: Seismic Time/Depth pair tracks the Checkshot Time/Depth Pairs, as an Evidence of accurate Calibration.

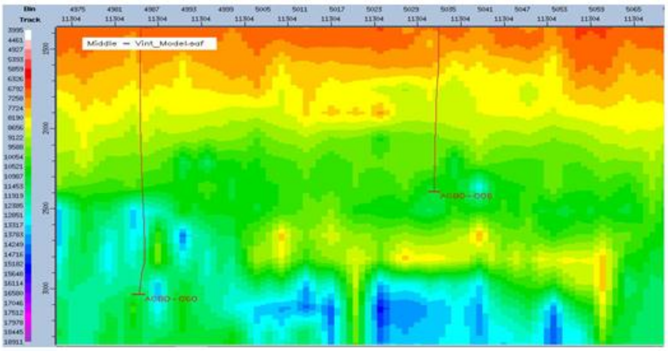

Fig. 5: The final Earth Model Velocity at the Offset Well Common Depth Point.

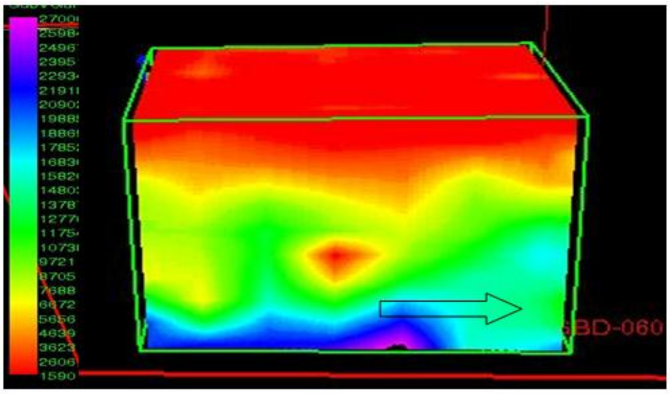

Fig. 6: Overburden Pressure Cube (Arrow indicates a slight drop in overburden pressure around the well trajectory).

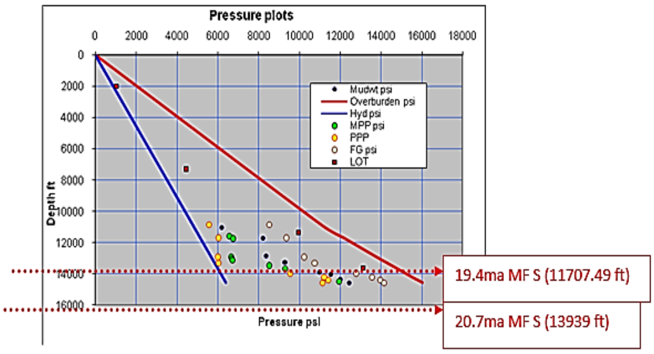

Fig. 7: Pore Pressure Profile for the Calibration Well, predicted from Valid Shale Intervals.

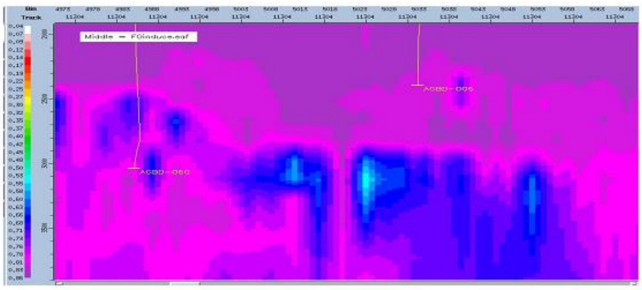

Fig. 8: The Fracture Gradient Profile of the Study Area derived from Seismic Velocities.

J. U. Okey, O. A. Davies, and V. Baatee, "Pre-Drill Pore Pressure Prediction from Seismic Velocities: A Case Study of Agbada Field in Niger Delta, Nigeria," *International Research Journal of Advanced Engineering and Science*, Volume 6, Issue 3, pp. 295-301, 2021.

International Research Journal of Advanced Engineering and Science
ISSN (Online): 2455-9024

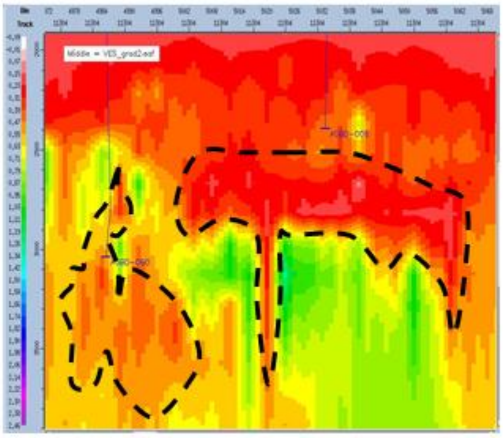

Fig. 9: Seismic derived VES Model for the Study Area (The regions marked with broken circles have overpressures. And these are between 2.5 to 3.5 seconds or 10,000 ft to 14,000 ft.)

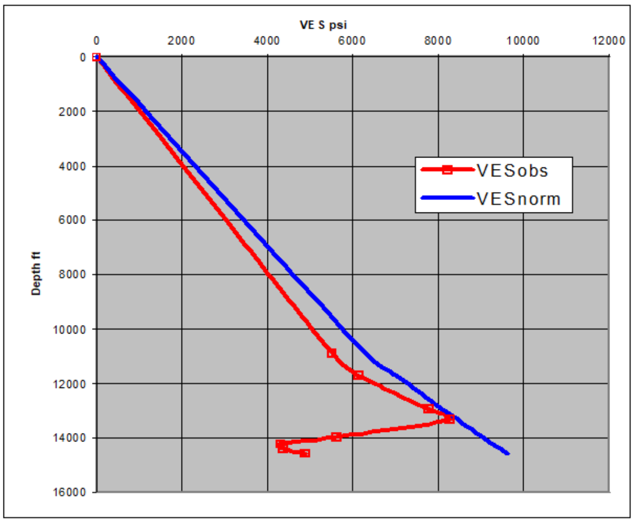

Fig. 10: VES versus Depth Plot from the well. (The major reversal around 13,600ft corresponds to the start of hard overpressures. A minor reversal can also be seen from 10,000ft to 11,800ft.)

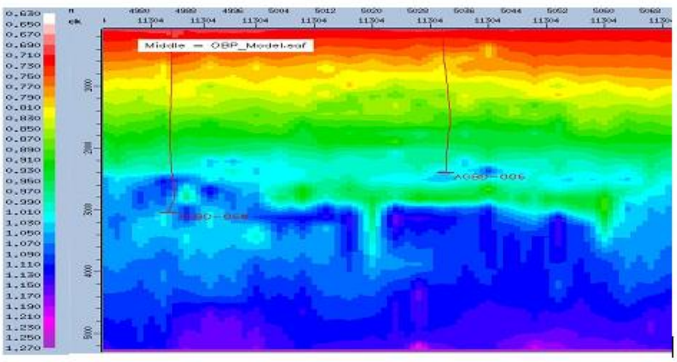

Fig. 11: Seismically Predicted Overburden Pressure Gradient

B. Discussions

The main objective of this research is to use seismic velocities to predict pore pressures prior to drilling. But this can only be done, if the velocities are sensitive to changes in vertical effective stress as much as well sonic velocities do [31, 32]. This necessitated the calibration of the seismic velocities with data obtained from the control well (Agb 60) in the vicinity of the project area.

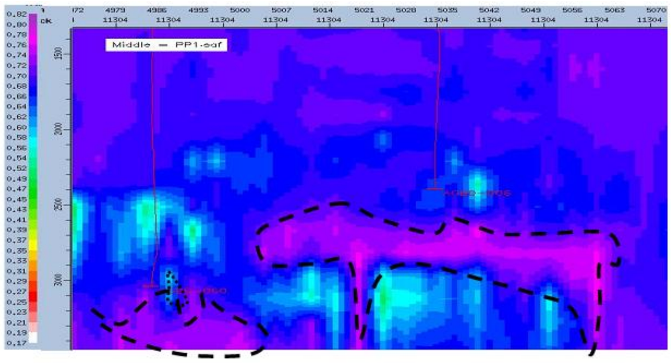

Fig. 12: Final 2D Pore Pressure Profile of the Study Area derived from Seismic Velocities

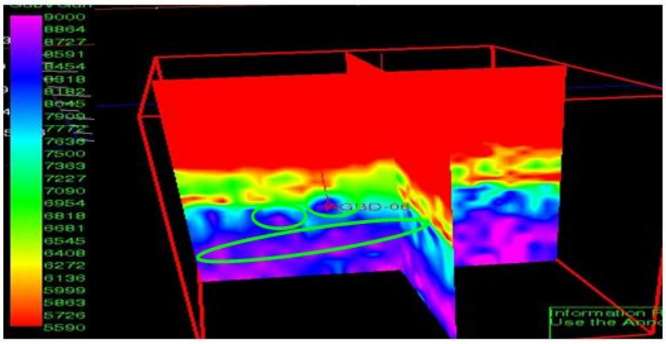

Fig. 13: The Final 3D Pore Pressure Model derived from Seismic Interval Velocities. (The circled areas are overpressured)

The control well is a deep well, with total depth of 14,508ftss originally drilled to test deep prospects in a rollover anticline structure, approximately between 12,000 and 15,500ftss deep. The estimated shale pressures show a normal hydrostatic trend from the top down to 10,800ftss, where a transition to overpressure was noticed, as shown in figure 7. The pressure increased in a step-wise manner down to about 11,702ftss. A drop in the predicted shale pressure of about 23psi was noticed between 11,703ftss and 13,318ftss. According to Barton and Moos [33], this could be likely due to leakage across bounding fault induced by production from the hydrocarbon bearing P650 paralic sequence in the adjacent Okpodon field, 10km north of the control well. This drop was also noticed in the reservoir, but of a much higher magnitude (800psi) and was responsible for the stuck pipe event at 13,038ft which led to the sidetrack introduced in the drilling of the well. The pressure transition zone for this area can be said to be between 10,887ftss to 11702ftss, where mild overpressures ranging from about 0.51psi to 0.52psi were observed. The top of geopressure is found at approximately 13,318ftss, from where hard overpressures ranging from 0.77 to 0.79psi occurred in the shale and much higher in the reservoirs.

As can be seen in figure 7, two regional marker shale (maximum flooding surfaces) control the over-pressures in the area; 19.4ma MFS (11707ftss) and 20.7ma MFS (13934ftss).

Additionally, there is a significant disparity between the reservoir pressures and the estimated shale pressures. This could be attributed to two factors; first, the well was drilled on a structural high, secondly, buoyancy effects due to the presence of hydrocarbon in some units of the adjacent reservoirs. There seem to be a centroid depth around 14,208 ftss, which might also be another factor. Usually above the centroid depth, the pore pressure in the sands exceeds that of the bounding shale [34, 35]. At the crest of a structure, the pore pressure in the sands can track the fracture gradient, thereby making it extremely difficult to drill, according to Dusseault et. al. [36].

The result of the well to seismic calibration indicates a perfect match especially at the intervals where well control exists. This can be seen clearly in figure 4. The seismically predicted fracture gradient tallies with those estimated from the calibration well as shown in figure 8, where a jump in values was observed between 2.8 and 3.0 seconds on the two-way seismic travel time which corresponds roughly to about 13,800ft. This depth is the onset of hard overpressures in the area. The final vertical effective stress model predicted from the seismic velocities shows a good match as seen in figure 9 and figure 10.

The seismically predicted overburden profile for the study area (figure 11) shows a slight drop between the intervals 2.8s and 3.0s in the calibration well Agb060, because of overpressures. Whereas at the vicinity well AGB-006, the overburden pressure is normal because there are no overpressure issues there. The OBP gradient values range from 0.9 to 1.1psi within the well control regions as seen in the well.

The predicted pore pressure profile from seismic velocities is shown in figure 12. The pressure trend agrees with the well, only within the depths where there are controls. The well log analysis started from approximately 10,000ft (2500ms) to the base of the well (14,560ft or 3650ms). As seen in the seismic pore pressure profile, the overpressure was mild between 2500ms and 2650ms. Afterwards, hard overpressures set in from 2700ms to 3100ms, with values hitting 0.82psi as seen by the well. But away from the calibration well, the vicinity well sits a few kilometers away (Agb006). From the well data, it was found to be normally pressured. This can also be confirmed from the seismic-derived pore pressure volume in figure 13 which tracks relatively accurately, the pore pressure events of the calibration well.

The VES profile, as well as the calibrated velocity profile, for the vicinity area also reveals that well Agb006 has no overpressure issues. But if drilling must be done below 2350ms which is the depth of Agb006, there will be a lot of hard overpressure issues to contend with, as seen in the pore pressure profile and in the VES and seismic velocity profiles. As a matter of fact, between 2500ms to 3100ms, hard overpressures pervade an extensive area, away from the calibration well.

V. Conclusion

The knowledge of pore pressure is a key requirement for optimal well development decisions in overpressure areas. This research was therefore embarked on to predict pore pressure profile ahead of drill bit, using seismic well log data from the Agbada field in the Niger Delta. The following conclusions were reached;

(i) Overpressures were encountered in the calibration well from 10,800ftss to 11,702ftss where mild over pressures of between 0.5 and 0.51psi were observed.
(ii) Hard overpressures of between 0.77 and 0.81psi were also seen from 13,318ftss to the bottom of the well at 14,502ftss.
(iii) From the well data, vertical effective stress reversal which is also an indicator of overpressure was observed at 11,702ftss. Another indicator of overpressure, overburden pressure, increased from 11,800ftss as well. The corresponding fracture gradient also increased at 14,000ftss.
(iv) The seismic derived fracture gradient increased between 2,800ms and 3,000ms (about 13,800ftss) in agreement with that calculated from the calibration well.
(v) Seismic-derived vertical effective stress reversal was also observed between 2,500ms and 3,500ms (10,000ftss – 14,000ftss), just as was observed in the well.
(vi) Seismic-derived overburden pressure dropped between 2,800ms and 3,000ms. This was also confirmed from the well results.
(vii) Mild overpressures were predicted from 2,500ms to 2,650ms (10,000ftss to 10,700ftss) and hard overpressure from 2,700ms to 3,100ms (11,000ftss to 13,200ftss).

Acknowledgment

The authors are grateful to Shell Petroleum Development Company (SPDC), Nigeria, for providing the data used for this research work.

References

[1] Cook, M., *Petroleum Economics and Risk Analysis: A Practical Guide to E&P Investment Decision-Making*. 2021: Elsevier.
[2] Speight, J.G., *Handbook of offshore oil and gas operations*. 2014: Elsevier.
[3] Leffler, W.L., G. Sterling, and R. Pattarozzi, *Deepwater petroleum exploration & production: a nontechnical guide*. 2011: PennWell Books, LLC.
[4] Sayers, C.M., *An introduction to velocity-based pore-pressure estimation.* The Leading Edge, 2006. 25(12): p. 1496-1500.
[5] Ghadimipour, A., H. Singh, and S. Perumalla. *Development of a Geomechanical Ranking System to Investigate Hydraulic Fracturing Feasibility of an Unconventional Shale Oil/Gas Reservoir: Case Study from Middle East*. in *SPE Middle East Oil and Gas Show and Conference*. 2019. OnePetro.
[6] Burley, S. and R. Worden, *Sandstone diagenesis: recent and ancient*. Vol. 24. 2009: John Wiley & Sons.
[7] Shaker, S., *Calibration of geopressure predictions using the normal compaction trend: Perception and pitfall.* CSEG Recorder, 2007. 32(01): p. 29-35.
[8] Fertl, W.H., *Abnormal formation pressures*. 1981: Elsevier.
[9] Genevois, R., P. Tecca, M. Berti, A. Simoni, E. Bromhead, N. Dixon, and M. Ibsen. *Pore pressure distribution in the initiation area of a granular debris flow*. in *Proceedings of the 8th International Symposium on Landslides, Cardiff*. 2000.
[10] Shaker, S.S. and D.J. Reynolds. *Kicks and Blowouts Prediction Before and During Drilling in the Over-Pressured Sediments*. in *Offshore Technology Conference*. 2020. OnePetro.

[11] Chopra, S. and A.R. Huffman, *Velocity determination for pore-pressure prediction.* The Leading Edge, 2006. 25(12): p. 1502-1515.
[12] Umoren, E.B., E.D. Uko, I. Tamunobereton-Ari, and C. Israel-Cookey, *Seismic Velocity Analysis for Improved Geopressure Modelling in Onshore Niger Delta.* International Journal of Advanced Geosciences, 2019. 7(2): p. 179-185.
[13] Umoren, E.B., A.O. Akankpo, K.I. Udo, O.I. Horsfall, J.G. Atat, and J. Asedegbega, *Velocity-Induced Pitfalls in Pore Pressure Prediction: Example from Niger Delta Basin, Nigeria.* Journal of Applied Geology and Geophysics, 2020. 8(1): p. 52-58.
[14] Baouche, R., S. Sen, M. Sadaoui, K. Boutaleb, and S.S. Ganguli, *Characterization of pore pressure, fracture pressure, shear failure and its implications for drilling, wellbore stability and completion design–a case study from the Takouazet field, Illizi Basin, Algeria.* Marine and Petroleum Geology, 2020. 120: p. 104510.
[15] Davies, D.H., O.A. Davies, and O.I. Horsfall, *Determination of Geomechanical Properties of a typical Niger Delta Reservoir Rock Using Geophysical Well Logs.* Asian Journal of Applied science Technology, 2019. 3(1): p. 222-233.
[16] Alao, O., W. Ofuyah, and A. Abegunrin, *Detecting and predicting over pressure zones in the Niger Delta, Nigeria: a case study of Afam Field.* Journal of Environment and Earth Science, 2014. 4(6): p. 13-20.
[17] Ajanaku, B. and O. Akintorinwa, *Determination of gas reservoir (s) using AVO inversion within "XY" field offshore Niger Delta.* Petroleum Research, 2019. 4(1): p. 52-58.
[18] Martin, A.K., C.J. Hartnady, and S.W. Goodlad, *A revised fit of South America and south central Africa.* Earth and Planetary Science Letters, 1981. 54(2): p. 293-305.
[19] Magbagbeola, O.A. and B.J. Willis, *Sequence stratigraphy and syndepositional deformation of the Agbada Formation, Robertkiri field, Niger Delta, Nigeria.* AAPG bulletin, 2007. 91(7): p. 945-958.
[20] Omnes, G. and P. Renoux, *Implications and findings associated with tying surface seismic to wells*, in *SEG Technical Program Expanded Abstracts 1993*. 1993, Society of Exploration Geophysicists. p. 147-149.
[21] Zhang, J., *Pore pressure prediction from well logs: Methods, modifications, and new approaches.* Earth-Science Reviews, 2011. 108(1-2): p. 50-63.
[22] Robinson, E. and C. Coruh, *Basic Exploration Geophysics, John Willey & Sons.* New York, 1988: p. 562.
[23] Eaton, B.A., *The effect of overburden stress on geopressure prediction from well logs.* Journal of Petroleum Technology, 1972. 24(08): p. 929-934.
[24] Nwozor, K.N., M.L. Omudu, B.M. Ozumba, C.J. Egbuachor, A.G. Onwuemesi, and A. O.L., *Quantitative Evidence of Secondary Mechanisms of Overpressure Generation: Insights from Parts of Onshore Niger Delta, Nigeria.* Petroleum Technology Development Journal, 2013. 3(1): p. 64-83.
[25] Asquith, G.B., D. Krygowski, and C.R. Gibson, *Basic well log analysis.* Vol. 16. 2004: American association of petroleum geologists Tulsa, OK.
[26] Terzaghi, K., *Theoretical soil mechanics. johnwiley & sons.* New York, 1943: p. 11-15.
[27] Dubose Jr, J.B., *A technique for stabilizing interval velocities from the Dix equation.* Geophysics, 1988. 53(9): p. 1241-1243.
[28] Gardner, G., L. Gardner, and A. Gregory, *Formation velocity and density—The diagnostic basics for stratigraphic traps.* Geophysics, 1974. 39(6): p. 770-780.
[29] Holbrook, P., D. Maggiori, and R. Hensley, *Real-time pore pressure and fracture gradient evaluation in all sedimentary lithologies.* SPE Formation Evaluation, 1995. 10(04): p. 215-222.
[30] King Hubbert, M. and W.W. Rubey, *Role of fluid pressure in mechanics of overthrust faulting: I. Mechanics of fluid-filled porous solids and its application to overthrust faulting.* Geological Society of America Bulletin, 1959. 70(2): p. 115-166.
[31] Lubanzadio, M., N. Goulty, and R. Swarbrick, *Dependence of sonic velocity on effective stress in North Sea Mesozoic mudstones.* Marine and Petroleum Geology, 2006. 23(6): p. 647-653.
[32] Kozlowski, K., M. Da Silva, D. Brown, J. Taylor, H. Willems, T. Watson, D. Burch, T. Hutton, C. Christensen, and M. Manohar. *The Importance of Overburden and Pore Pressure on Horizontal Stress Magnitude Determination; an Example From the Delaware Basin*. in *Unconventional Resources Technology Conference, Houston, Texas, 23-25 July 2018*. 2018. Society of Exploration Geophysicists, American Association of Petroleum Geophysicist.
[33] Barton, C. and D. Moos, *Geomechanical wellbore imaging: key to managing the asset life cycle.* AAPG Memoir, 2010. 92: p. 81–112.
[34] Kaeng, G.C., S. Sausan, and A. Satria. *Geopressure Centroid as Pore Pressure Prediction Challenge in Deepwater South East Asia*. in *International Petroleum Technology Conference*. 2014. OnePetro.
[35] Schofield, N., S. Holford, and A. Edwards, *Overpressure transmission through igneous intrusions: An unrecognized drilling hazard in volcanic affected basins?* ASEG Extended Abstracts, 2019. 2019(1): p. 1-5.
[36] Dusseault, M.B., V. Maury, F. Sanfilippo, and F.J. Santarelli. *Drilling around salt: risks, stresses, and uncertainties*. in *Gulf Rocks 2004, the 6th North America Rock Mechanics Symposium (NARMS)*. 2004. OnePetro.